JOURNAL OF BACTERIOLOGY, July 2005, p. 4410–4420 Vol. 187, No. 13
0021-9193/05/$08.00+0 doi:10.1128/JB.187.13.4410–4420.2005

Coupling of NAD^+ Biosynthesis and Nicotinamide Ribosyl Transport: Characterization of NadR Ribonucleotide Kinase Mutants of *Haemophilus influenzae*

Melisa Merdanovic, Elizabeta Sauer, and Joachim Reidl*

Institut für Hygiene und Mikrobiologie, Universität Würzburg, Josef Schneider Str. 2, E1, 97080 Würzburg, Germany

Received 3 February 2005/Accepted 21 March 2005

Previously, we characterized a pathway necessary for the processing of NAD^+ and for uptake of nicotinamide riboside (NR) in *Haemophilus influenzae*. Here we report on the role of NadR, which is essential for NAD^+ utilization in this organism. Different NadR variants with a deleted ribonucleotide kinase domain or with a single amino acid change were characterized in vitro and in vivo with respect to cell viability, ribonucleotide kinase activity, and NR transport. The ribonucleotide kinase mutants were viable only in a *nadV*$^+$ (nicotinamide phosphoribosyltransferase) background, indicating that the ribonucleotide kinase domain is essential for cell viability in *H. influenzae*. Mutations located in the Walker A and B motifs and the LID region resulted in deficiencies in both NR phosphorylation and NR uptake. The ribonucleotide kinase function of NadR was found to be feedback controlled by NAD^+ under in vitro conditions and by NAD^+ utilization in vivo. Taken together, our data demonstrate that the NR phosphorylation step is essential for both NR uptake across the inner membrane and NAD^+ synthesis and is also involved in controlling the NAD^+ biosynthesis rate.

A well-known physiological hallmark of *Haemophilus influenzae* is the lack of de novo biosynthetic pathways for two essential cofactors, hemin (factor X) and NAD^+ (factor V) (8). The NAD^+ dependence was described decades ago, and it was shown that NAD^+ or a precursor, such as nicotinamide riboside (NR) or nicotinamide mononucleotide (NMN), must be present in the growth medium for cell propagation (6, 14, 45). Other related species, such as *Haemophilus aphrophilus*, *Haemophilus ducreyi*, and *Pasteurella* and *Actinobacillus* spp., can utilize nicotinamide (Nam) and are therefore referred to as factor V independent (24). Enzymatic activities for NAD^+ degradation and resynthesis have been described for *H. influenzae* and *Haemophilus parainfluenzae*. These activities include NAD^+ pyrophosphatase (21), nicotinamide ribonucleoside kinase (RNK), NMN adenylyltransferase (NMNAT), nucleoside phosphorylase, NAD^+ kinase, and NAD^+ glycohydrolase (6, 7). Not long ago, it was found that eukaryotic cells also possess an RNK activity (43), and only recently it was found that NR is a substrate (4); therefore, NAD^+ resynthesis can occur via a Preiss-Handler independent route in eukaryotes. There is increasing interest in this field since NR may be considered an important nutrient factor and because the NR pathway seems to be involved in activation of nucleotide antitumor prodrugs, such as benzamide riboside, tiazofurin, and selenazofurin (4, 43).

As shown recently, the amino acid sequence of NadR of *Escherichia coli* has a motif that is also found in adenylyltransferases, and it has been demonstrated that NadR possesses NMNAT activity (38). Moreover, the NadR homologue of *H. influenzae* was found to possess RNK activity (27). Structural and biochemical analysis proved that the NMNAT motif is located in the N′-terminal half of the NadR protein, whereas the RNK domain is located in the C′-terminal half (46). The RNK domain contains Walker A (P-loop) and Walker B motifs responsible for ATP binding and hydrolysis, respectively (27, 46, 49). In addition, a proposed LID domain was identified. LID domains have been found in other kinases (31), and these domains are regions which are able to move after substrate binding (34, 54) and are responsible for coordination of three distinct conformations, an open state in the absence of substrate, a partially closed state after substrate binding, and a closed state if both substrates are present (29).

NadR was first described as a transcriptional regulator protein that acts as a repressor for several genes needed for de novo NAD^+ biosynthesis and pyridine nucleotide cycles in *Salmonella enterica* serovar Typhimurium (11, 36, 56). The function of NadR is to integrate the signals of NAD^+ starvation. Under nonstarvation conditions NadR is bound with its corepressor, NAD^+, and this leads to DNA binding activity that represses the transcription of *nadA*, *nadB*, and *pncB* (10). In the presence of a decreased concentration of NAD^+, association between NadR and ATP seems to take place, and an NadR-ATP complex does not act as a repressor (37). Furthermore, it was assumed that an NadR-ATP complex activates NMN uptake via the PnuC transporter (36). Mutations which interfered with NMN uptake were obtained in the C′-terminal part of NadR (12). However, so far there are no direct data which explain how NadR interacts with or activates the PnuC permease function.

A helix-turn-helix DNA binding domain present in NadR of *S. enterica* serovar Typhimurium (12) could not be found in the NadR homologue of *H. influenzae*. Therefore, it was proposed that in *H. influenzae* NadR has no regulatory function at the transcriptional level (27). In *H. influenzae*, NR enters the NAD^+ resynthesis pathway after uptake, NR is phosphorylated to obtain NMN by a nicotinamide RNK activity, and

* Corresponding author. Mailing address: Institut für Hygiene und Mikrobiologie, Universität Würzburg, Josef Schneider Str. 2, E1, 97080 Würzburg, Germany. Phone: 49 931 20146159. Fax: 49 931 20146445. E-mail: joachim.reidl@mail.uni-wuerzburg.de.

subsequently, NAD^+ is synthesized from NMN and ATP via an NMNAT activity (6, 27). Summarizing these features, NadR represents an amazing multifunctional regulator/enzyme complex able to integrate several features, such as enzymatic, transport, and transcriptional (regulatory) activities.

The NadR reaction starts with NR, and recently, the components of the *H. influenzae* pathway necessary for NAD^+, NMN, and NR uptake were determined. We characterized two enzymes, a nucleotide phosphatase encoded by the *e*(P4) outer membrane protein and NadN, an NAD^+ nucleotidase located in the periplasm (23, 40, 44). In addition, we showed that NAD^+ and NMN cross the outer membrane mainly via the OmpP2 porin (2). However, only NR can be utilized by the transport system located in the inner membrane (19, 42), which is encoded by a homologue of *pnuC*. We characterized the *pnuC* gene product as the protein that is responsible for the main flow of the NR substrate into the cytoplasm, and we also found that *H. influenzae pnuC* knockout mutants were not able to grow under in vivo conditions (there was not invasive growth in infected infant rats) (19).

In this study, we investigated the *nadR* homologue gene product (HI0763) (9) of *H. influenzae*. In particular, we studied its role as an essential gene product for cell viability, the correlation of RNK activity, NR uptake, and negative feedback regulation. Based on the recent identification of spontaneous *nadR* mutants, which provide 3-aminopyridine resistance (42), and the published structure of NadR (46), we generated site-directed *nadR* mutants and tested them to determine their effects on NR transport and NAD^+ synthesis. We showed indirectly that an impaired RNK function of NadR results in nonviable cells, which demonstrated that the RNK domain is essential for growth of *H. influenzae* and that the RNK activity determines NR transport. Furthermore, we showed that RNK activity is negatively regulated by NAD^+ feedback inhibition and obtained evidence that NR uptake is under NadR feedback control. Therefore, we postulate that intracellular NAD^+ concentrations control the uptake of NR and NAD^+ biosynthesis.

MATERIALS AND METHODS

Bacterial strains, plasmids, and growth media. Strain *H. influenzae* Rd KW20 was obtained from A. Wright (Tufts University, Boston, Mass.). This strain was manipulated to contain the *sxy-1* mutation (39), which made it constitutively competent and yielded AK01, as reported recently (42). Strain AK01 was used for all genetic manipulations. In general, *H. influenzae* strains (Table 1) were cultured in brain heart infusion (BHI) broth (Merck, Darmstadt, Germany) or on BHI agar supplemented with NAD^+ (15 μM) or NR (15 μM) and hemin (10 μg/ml). Antibiotics were used as described by Barcak et al. (3), except that the concentration of chloramphenicol was 0.5 μg/ml. *E. coli* K-12 strains (Table 1) were cultured in Luria-Bertani (LB) broth (Merck, Darmstadt, Germany) or on LB agar plates. Kanamycin (50 μg/ml) or chloramphenicol (30 μg/ml) was added for selection of transformants using kanamycin. *E. coli* strains ER2566 (New England Biolabs, Schwalbach, Germany) and TOP10F′ (Invitrogen) were employed for cloning plasmid constructs. BL21/pLysS (Invitrogen) was used for protein expression.

DNA purification, hybridization, PCR, and DNA sequencing. Isolation and preparation of chromosomal DNA were done by using the method of Grimberg et al. (15). DNA hybridization and blotting were performed as described by Southern (47). Briefly, chromosomal DNA was digested with restriction enzymes, separated on an agarose (0.7%) gel, and transferred to a Hybond N^+ membrane (Amersham Pharmacia Biotech, Freiburg, Germany). DNA probe labeling and hybridization were performed according to the manufacturer's instructions with an ECL direct nucleic acid labeling and detection kit (Amersham Pharmacia Biotech). PCRs for sequencing and subcloning were carried out using the TripleMaster system (Eppendorf, Hamburg, Germany). DNA sequencing was performed with an ABI 310 genetic analyzer (Applied Biosystems, Weiterstadt, Germany).

NadR mutant construction. For deletion construction of the RNK domain of NadR (amino acids 225 to 410), two PCR DNA fragments were generated. One fragment was amplified with oligonucleotides RNK1EcoRI5′ and RNK2PstI3′ (Table 2), which generated a 374-bp fragment of *nadR* starting from position 252 located downstream of the annotated start codon. The second PCR fragment was generated with oligonucleotides nadR3PstI5′ and nadR4HindIII (Table 2), which generated a 701-bp fragment starting from position 1225 located in *nadR* and extending into the next open reading frame, HI0762. The PCR products were digested with PstI, EcoRI, and HindIII (Table 2) and ligated with a PstI-digested *cat* gene cassette (26) and with an EcoRI- and HindIII-digested pUC19 plasmid (55). The ligation mixture was transformed into *E. coli* ER2566. Chloramphenicol-resistant (Cm^r) clones were isolated, and one of them was further tested and found to contain a *cat* gene inserted in the same transcriptional orientation as *nadR*, which was verified by DNA sequencing (data not shown). This plasmid was designated pUCΔRNK. For *nadR* RNK domain deletion construction pUCΔRNK was used as the template to amplify the *nadR′-cat-′HI0762* gene fragment using oligonucleotides RNKEcoRI and nadRHindIII (Table 2). PCR amplification resulted in a 2,063-bp fragment, which was gel purified (QIAGEN, Hilden, Germany) and transformed into strain SE01 (42). This construction resulted in deletion of amino acids 225 to 410 of NadR in strain SE01ΔRNK.

An additional *nadR* deletion mutant, SE01*nadR*Δ58::*cat*, which lacked the C′-terminal 58 amino acids (amino acids 352 to 410), was generated. For mutant construction, we used the strategy described above with oligonucleotides X1-EcoRI and nadRΔ58-2PstI5′ upstream of the region and oligonucleotides nadR3PstI5′ and nadR4HindIII downstream of the region (Table 2). Transformation was carried out as described previously (19), and transformed cells were plated on BHI agar supplemented with chloramphenicol. After 48 h of growth, Cm^r colonies were obtained and purified. Chromosomal DNA was prepared, and the *cat* insertion into the chromosomal *nadR* locus was verified by Southern blot analysis using the entire *cat* and *nadR* genes as labeled probes (data not shown).

An *nadR* complementation plasmid was constructed by generating an *nadR* DNA fragment with oligonucleotides nadRKpnIup2 and nadRKpnIdown (Table 2). This PCR fragment contained the *nadR* gene, as annotated in The Institute for Genome Research database, with GTG as an alternative start codon (9). After PCR amplification this 1,288-bp DNA fragment was digested with KpnI and ligated into a KpnI-digested pSSkanΔcm plasmid that was a derivative of pZA31-luc (32), in which the *cat* gene was deleted (Table 2). Kan^r clones were verified by DNA restriction and sequencing (data not shown). The resulting plasmid was designated pNadRkan.

Construction of an *nadR* His-tagged expression system. The full-size *nadR* gene (annotated sequence according to Fleischmann et al. [9]) was amplified with primers nadRtopoI5′ and nadRtopo3′ (Table 2) using genomic DNA as the template and TripleMaster Mix proofreading polymerase. The PCR fragment was purified and ligated into the pCRT7/CT-TOPO plasmid, and the ligation mixture was transformed into competent *E. coli* TOP10F′ according to the manufacturer's instructions (Invitrogen), resulting in plasmid pMMnadR-His_6, in which the C terminus of *nadR* carried V5 and His_6 tags. The correct *nadR* sequence was confirmed by sequencing, and plasmid pMMnadR-His_6 was used for NadR-His purification and as a template for site-directed mutagenesis.

Site-directed mutagenesis. The primers used for mutagenesis were designed to contain a specific restriction site either directly at or near the nucleotide position coding for the amino acid that was substituted (triplets coding for substituted amino acids and restriction sites are shown in Table 2). Using pMMnadR-His_6 as a template and starting from the site of substitution, the entire plasmid was amplified by PCR. The resulting product was purified, digested with appropriate restrictions enzymes, relegated, and transformed into *E. coli* TOP10F′. Transformants with plasmids carrying mutated *nadR* genes (Table 1) were confirmed by digestion with appropriate enzymes and DNA sequencing (data not shown).

For transformation of recombinant *nadR*-His_6 into *H. influenzae* strain SE01ΔRNK, pMMnadR-His_6 was digested with XbaI and PmeI. The 1,404-bp fragment carrying the *nadR*-His_6 gene sequence was gel purified and cloned into NheI/EcoRV-digested pBAD18Kan (16). The resulting plasmid was designated pBADnadR-His and used for transformation of the *nadR*-His_6 gene into *H. influenzae*. pUC-derived plasmids cannot replicate in *H. influenzae* (3), and therefore pBAD18Kan is a suicide plasmid for this species. After transformation of pBADnadR-His, the cells in which the plasmid had integrated into the remaining *nadR* portion of the *nadR*ΔRNK::*cat* locus via single homologous recombination were selected by growth on kanamycin-containing agar. The colonies had a single chromosomal copy of *nadR*-His_6 under control of the promoter and the ribosomal binding site of the native NadR. Correct integration of the pBADnadR-His plasmid into the *nadR* locus on the chromosome was confirmed by Southern

TABLE 1. Relevant strains and plasmids used in this study

Strain or plasmid	Relevant phenotype and/or genotype	Source or reference
Escherichia coli strains		
TOP10F	F′ [*laqI*^{q} Tn*10*(Tc^r)] *mcrA* Δ(*mrr-hsdRMS-mcrBC*) ϕ80*lacZ*ΔM15 Δ*lacX74 recA1 deoR araD139* Δ(*ara-leu*) *galU galK rpsL* (Sm^r) *endA1 nupG*	Invitrogen
BL21 (DE3)/pLysS	F$^-$ *ompT hsdS*$_B$ (r_B^- m_B^-) *gal dcm* (DE3)/pLysS (Cm^r)	Invitrogen
ER2566	*fhuA2 (lon) ompT lacZ*::T7 *gene1 gal sulA11* Δ(*mcrC-mrr*)*114*::IS*10* R(*mcr-73*::mini-Tn*10*-Tet^s)2 R(*zgb-210*::Tn*10*)(Tet^s) *endA1*(*dcm*)	New England Biolabs
Haemophilus influenzae strains		
Rd KW20	Genome determined	9
AK01	Strain Rd (*sxy-1* Strep^r) constitutive competent	18
SE01	*nadV*, Nam$^+$	42
SE01ΔRNK	*nadR*ΔRNK::*cat*, Nam$^+$ Cm^r	This study
SE01ΔRNK58	*nadR*Δ58RNK::*cat*, Nam$^+$ Cm^r	This study
SE02ΔRNK	SE01ΔRNK *nadR*::pBADnadR-His, Kan^r	This study
SE03ΔRNK	SE01ΔRNK *nadR*::pBADnadR(G^{238}N), Kan^r	This study
SE04ΔRNK	SE01ΔRNK *nadR*::pBADnadR(G^{238}S), Kan^r	This study
SE05ΔRNK	SE01ΔRNK *nadR*::pBADnadR(D^{238}C), Kan^r	This study
SE06ΔRNK	SE01ΔRNK *nadR*::pBADnadR(D^{238}N), Kan^r	This study
SE07ΔRNK	SE01ΔRNK *nadR*::pBADnadR(D^{238}S), Kan^r	This study
SE08ΔRNK	SE01ΔRNK *nadR*::pBADnadR(R^{238}C), Kan^r	This study
SE09ΔRNK	SE01ΔRNK *nadR*::pBADnadR(R^{238}M), Kan^r	This study
SE10ΔRNK	SE01ΔRNK *nadR*::pBADnadR(R^{238}N), Kan^r	This study
SE11ΔRNK	SE01ΔRNK *nadR*::pBADnadR(W^{256}F), Kan^r	This study
SE12ΔRNK	SE01ΔRNK *nadR*::pBADnadR(Y^{292}I), Kan^r	This study
SE13ΔRNK	SE01ΔRNK *nadR*::pBADnadR(K^{126}A), Kan^r	This study
SE14ΔRNK	SE01ΔRNK *nadR*::pBADnadR(K^{126}T), Kan^r	This study
Plasmids		
pACYC184	Cm^r Tet^r	New England Biolabs
pACYC184nadR(His$_6$)	Tet^r	This study
pMMnadR-His$_6$	Amp^r; *nadR*-C′-terminal His tagged	42
pUCΔRNK	Cm^r Amp^r, *nadR*::*cat*::*nadR′*	This study
pSSkan	Kan^r Cm^r	S. Schild
pSSkanΔcm	pSSkan, Cm^s Kan^r	This study
pNadRkan	pSSkanΔcm, *nadR*$^+$	This study
pBAD18-Kan	Kan^r	16
pBADnadR-His	Kan^r, *nadR*-C′-terminal His tagged	This study
nadR point mutants		
pBADnadR(G^{238}N)-His$_6$	Kan^r	This study
pBADnadR(G^{238}S)-His$_6$	Kan^r	This study
pBADnadR(D^{304}C)-His$_6$	Kan^r	This study
pBADnadR(D^{304}N)-His$_6$	Kan^r	This study
pBADnadR(D^{304}S)-His$_6$	Kan^r	This study
pBADnadR(R^{352}C)-His$_6$	Kan^r	This study
pBADnadR(R^{352}M)-His$_6$	Kan^r	This study
pBADnadR(R^{238}N)-His$_6$	Kan^r	This study
pBADnadR(W^{256}F)-His$_6$	Amp^r	This study
pBADnadR(Y^{292}I)-His$_6$	Amp^r	This study
pBADnadR(K^{126}A)-His$_6$	Amp^r	This study
pBADnadR(K^{126}T)-His$_6$	Amp^r	This study
pMMnadR(G^{238}N)-His$_6$	Amp^r	This study
pMMnadR(G^{238}S)-His$_6$	Amp^r	This study
pMMnadR(D^{304}C)-His$_6$	Amp^r	This study
pMMnadR(D^{304}N)-His$_6$	Amp^r	This study
pMMnadR(D^{304}S)-His$_6$	Amp^r	This study
pMMnadR(R^{352}C)-His$_6$	Amp^r	This study
pMMnadR(R^{352}M)-His$_6$	Amp^r	This study
pMMnadR(R^{238}N)-His$_6$	Amp^r	This study
pMMnadR(W^{256}F)-His$_6$	Amp^r	This study
pMMnadR(Y^{292}I)-His$_6$	Amp^r	This study
pMMnadR(K^{126}A)-His$_6$	Amp^r	This study
pMMnadR(K^{126}T)-His$_6$	Amp^r	This study

blotting and DNA sequencing of PCR-generated *nadR* (data not shown). All point mutations in the *nadR*-His$_6$ tagged gene were subcloned into pBAD18kan (Table 1) and were subsequently transferred into strain SE01ΔRNK as described above.

NadR His-tagged protein purification. The NadR His-tagged protein was expressed in the BL21(DE3)/pLysS strain of *E. coli* as a C′-terminal V5/His$_6$ fusion protein. Cultures (400 ml) were grown in LB medium with ampicillin (100 μg/ml) at 37°C with shaking to an optical density at 600 nm (OD_{600}) of 0.8. The temperature was adjusted to 18°C, and expression was induced with isopropyl-β-D-thiogalactopyranoside (IPTG) (0.8 mM). Cells were harvested after 18 h of shaking at 18°C. Cells were washed and resuspended in 4 ml of NaH_2PO_4 (50 mM)–NaCl (300 mM), pH 8, containing mercaptoethanol (2 mM), Brij 35 (0.03%), and a protease inhibitor mixture (Complete, EDTA-free; Boehringer, Ingelheim, Germany). The cells were opened with a French press, and the lysate

TABLE 2. Oligonucleotides used in this study

Oligonucleotide	Sequence (5′ to 3′)[a]
Oligonucleotides used for cloning	
RNK1EcoR15′	AGATTGAATTCCGCATGCCAACCGTGCAAGATC
RNK2Pst123′	AATCTGCAGCACCGTTTTGGCTTA GAAAGGACGAGC
nadR3Pst15′	AATCTGCAGTACAAAACACAACCTTTCC
nadR4HindIII	CAAAAGCTTCGTGATGATGTCCGTGGAATAC
XI-EcoR1	GATGAATTCTCTGACTATCCGCAAATGGC
nadRΔ582Pst1	TTTACTGCAGACGCAAGCCATCATCCACCCATTC
nadRKpn1up2	GAAATGGTACCGTGGGCTTTACCACCGGTAG
nadRKpn1down	AATAAGGTACCGTGCGGATCACCAGCAAAT
nadRtopo15′	GTGGGCTTTACCACCGGTAGGGAAT
nadRtopo3′	TTGAGATGTCCCTTTTATAGGAAAG
Oligonucleotides used for site-directed mutagenesis	
LIDnadRR352C 5′	ATTATC**TGC**AGCTTAGGCTCACAAAAACAACGC
LIDnadRR352C 3′	CTAAAGCT**GCA**GAGGCCATCATCCACCCATTC
LIDnadRR352M 5′	ACTGAATGGGTGGATGATGGGCTC**ATG**AGCTTA
LIDnadRR352M 3′	AGCCTAAGCT**CAT**GAGCCCATCATCCACC
LIDnadRR352N 5′	GAAGCTG**AAT**TCATTAGGCTCACAAAAACAACGC
LIDnadRR352N 3′	AAATTGA**ATT**CAGGCCATCATCCACCCATTCAGTAT
WalkerBnadRD304C	AATTTATCATA**TGC**ACGGATTTCATCACCACGCAAGCATTC
WalkerBnadRD304C 3′	TTTC**GCA**CATATGAATGCAATTTTATGAGAATGGCGCAC
WalkerBnadRD304N 5′	AAAATTTATAA**AT**ACGGATTTCATCACCACGCAA
WalkerBnadRD304N 3′	AAAACGT**ATT**TATAAATGCAATTTTATGAGAATGGC
WalkerBnadRD304S 5′	AAATTTTATA**AGC**ACGGATTTCATCACCACGCAA
WalkerBnadRD304S 3′	AAAACGT**GCT**TATAAATGCAATTTTATGAGAATGGC
WalkerAnadRG238N 5′	AAAAGAGAGCTCT**AAC**AAAAGCGTGCTAGTTAAT
WalkerAnadRG238N 3′	AATTT**GTT**AGAGCTCTCTCCCCCTAAAATCGC
WalkerAnadRG238S 5′	AAATGAGAGCTCT**AGC**AAAAGCGTGCTAGTTAAT
WalkerAnadRG238S 3′	AAATTT**GCT**AGAGCTCTCTCCCCCTAAAATCGC
nadRK126A5	GCGTTGGATGCAGCAAATTTTC**GCA**TATCAAAAAAATCAGATTTTTATTCATC
nadRK126A 3′	GATGAATAAAAATCTGATTTTTTTGATA**TGC**GAAAATTTGCTGCATCCAACGC
nadR W256F 5′	GTATTTAATACCACTTCTGCG**TTC**GAATACGGGCGTGAATTTG
nadR W256F 3′	CAAATTCACGCCCGTATTC**GAA**CGCAGAAGTGGTATTAAATAC
nadR Y2921 EcoRV 5′	TTGAT**ATC**GCCGTGCGCCATTCTCATAAAATTGC
nadR Y2921 EcoRV 3′	GC**GAT**ATCAATGTATCGTTGATGACCAAGCGC

[a] Boldface type indicates triplets coding for point mutations, and restriction sites are underlined.

was centrifuged to remove the cell debris (10,000 × *g*, 4°C, 20 min). The supernatant was loaded onto a Protino 1000 column (Macherey-Nagel, Düren, Germany) that was equilibrated with the same buffer. The column was washed with starting buffer containing Brij 35 (0.3%), and the bound proteins were eluted with starting buffer containing imidazole (250 mM). Eluted fractions were analyzed by sodium dodecyl sulfate—12% polyacrylamide gel electrophoresis performed as described by Laemmli (28). Fractions containing NadR-His_6 were pooled and dialyzed against HEPES-NaOH (50 mM, pH 7.5), NaCl (200 mM), dithiothreitol (1 mM). Aliquots of protein samples were shock frozen with liquid nitrogen and stored at −80°C.

Generation of NadR antiserum. NadR antiserum was produced from rabbits at Biotrend Chemikalien (Köln, Germany) by immunization with purified His_6-tagged NadR (1 mg/ml). For immunoaffinity purification of the serum, 3 mg of NadR-His_6 was coupled to 1 ml of Affigel-10 beads (Bio-Rad) according to the recommendations of the manufacturer. Two milliliters of serum (preheated at 50°C for 30 min) was incubated with NadR-His_6-containing beads overnight at 6°C. The beads were transferred to a column and washed with 50 ml washing buffer (20 mM HEPES-NaOH, pH 7.5, 1 M NaCl, 10 mM $MgCl_2$). The NadR-specific immunoglobulins were eluted with 100 mM glycine (pH 2.5), 100 mM NaCl, 10 mM $MgCl_2$. The pH of the eluted immunoglobulins was adjusted to 7 by addition of 1 M Tris. Purified serum was aliquoted and stored at −20°C. For Western blotting purified NadR antiserum was used at a dilution of 1:100 in 10% milk powder. Detection was performed with an ECL detection kit (Amersham) using horseradish peroxidase-coupled goat anti-rabbit antibodies (Dianova, Hamburg, Germany) at a 1:7,000 dilution.

In vitro enzyme assay. To test for NMNAT and RNK activities of purified NadR, a radioactive assay was used. Assays were carried out with HEPES-NaOH (100 mM, pH 7.5) with $MgCl_2$ (10 mM) by using a 40-μl (final volume) mixture. Purified NadR samples (ca. 0.04 mg/ml) were incubated with [^{14}C]NR (40 μM) or [^{14}C]NMN (45 μM) and ATP (2 mM) at 37°C for 40 min. The reaction was stopped by incubating the samples for 3 min at 100°C. After this, the protein was removed by centrifugation (5 min, 13,000 rpm). The NAD^+ inhibition studies were carried out in a similar way, except that the NadR protein concentration was approximately 4 μg/ml. The concentration of NAD^+ (pH 7.0) was up to 9 mM, which was about 200-fold greater than the concentration of [^{14}C]NR or [^{14}C]NMN.

Nicotinamide nucleotide reagents. Carbonyl [^{14}C]NAD^+ (specific activity, 50 mCi/mmol) was obtained from Amersham Biosciences (Freiburg, Germany), and [^{14}C]NMN was prepared from carbonyl [^{14}C]NAD^+ by treatment with snake venom nucleotide pyrophosphatase (Sigma). [^{14}C]NR was prepared by incubating carbonyl [^{14}C]NAD^+ with snake venom nucleotide pyrophosphatase and alkaline phosphatase in alkaline phosphatase buffer for 1 h at 37°C. Enzymes were inactivated by heating the reaction mixture for 2 min at 100°C, and then the supernatants were recovered by centrifugation (5 min, 10,000 rpm).

Cell extracts. The cells were grown in BHI medium supplemented with hemin (10 μg/ml) and appropriate antibiotics at 37°C in shaking flasks to an OD_{490} of 1. Cells were harvested and washed with HEPES-NaOH (50 mM, pH 7.5), and then they were resuspended in 0.01 volume of ice-cold HEPES-NaOH (50 mM, pH 7.5) containing NaCl (50 mM) and EDTA-free protease inhibitor cocktail (La Roche Boehringer, Ingelheim, Germany) and opened with a French press. The lysate was centrifuged (20 min, 10,000 × *g*) to remove the cell debris. Subsequently, the supernatant was used as a crude cell extract. The crude cell extract was further fractionated for localization studies. To obtain a soluble cell fraction containing proteins, the crude cell extract was ultracentrifuged (30 min, 90,000 rpm, 4°C; TLA100 rotor; Beckmann TL-100 ultracentrifuge). The resulting pellet was resuspended in HEPES-NaOH (50 mM) containing NaCl (1 M) and incubated for 1 h at 4°C with gentle shaking, and this was followed by another ultracentrifugation step (see above). The supernatant contained the membrane-associated proteins. The pellet was then extracted with HEPES-NaOH (50 mM) containing Triton X-100 (2%) by overnight incubation with gentle shaking at 4°C. Ultracentrifugation (see above) was used to separate the Triton X-100-soluble membrane protein fraction from the nonsoluble material. Protein concentrations of cell extracts were determined as described by Bradford (5) with a Bio-Rad protein assay kit (Bio-Rad, Munich, Germany).

Whole-cell labeling with [^{14}C]NAD^+. *H. influenzae* cells were grown to an OD_{490} of 2 in BHI medium supplemented with hemin. After cells were harvested

by centrifugation (4,000 × *g*, 10 min), they were washed and resuspended in BHI broth without supplements, the OD_{490} was adjusted to 2, and the preparation was incubated at room temperature for 1 h. Aliquots (5 ml) were taken and labeled with [^{14}C]Nam (1 μM), [^{14}C]NR (1 μM), or [^{14}C]NAD$^+$ (1 μM). Duplicate samples (500 μl) were taken at defined time intervals. Samples were then washed twice with HEPES-NaOH (0.1 M) and NaCl (0.1 M) and then carefully resuspended in HEPES-NaOH (100 mM) and boiled (5 min, 100°C). The samples were centrifuged (10 min, 13,000 rpm), and the supernatants (10 μl) were spotted on thin-layer chromatography (TLC) plates.

Thin-layer chromatography. Radioactive labeled samples were separated by TLC with a solvent system consisting of ammonium acetate (1 M, pH 5) and ethanol (30:70) (22) using Cellulose F plates (Merck, Darmstadt, Germany). After separation, the plates were dried and exposed to radiation-sensitive film (Eastman Kodak Co., Rochester, N.Y.). Spots were identified by comparison with reference samples of carbonyl [^{14}C]NAD$^+$, [^{14}C]NMN, [^{14}C]NR, and [^{14}C]Nam.

[^{14}C]NAD$^+$ utilization studies. *H. influenzae* SE01 and different *nadR* mutants of SE01 derivatives (Table 1) and the *nadR*$^+$ complementing strain were grown to an OD_{490} of 2. After centrifugation (4,000 × *g*, 10 min), the pellets were washed and resuspended in BHI broth without supplements, washed, and resuspended to an OD_{490} of 2. Unless indicated otherwise, aliquots (2.5 ml) were incubated for 1 h at 37°C. [^{14}C]NAD$^+$ (1 μM) was added to cell samples, and aliquots (500 μl) were removed at defined time intervals. The samples were filtered through ME 25 filters (0.45 μm; Schleicher & Schuell, Dassel, Germany) which were presoaked in NaCl (0.1 M). The filters were washed with NaCl (0.1 M) and placed into vials containing scintillation liquid (5 ml; Emulsifier-Safe; Packard, Dreieich, Germany). Radioactivity was measured with a Tri-Carb 1500 scintillation counter (Packard, Frankfurt, Germany).

RESULTS

NR ribonucleotide kinase is essential. Based on a genomic survey, NadR was recently suggested to be a novel target for antimicrobial therapy development (13, 27). The essential role of NadR was demonstrated indirectly, by in vitro transposon insertions in *nadR* that could not be transferred onto the chromosome (1, 27). This result suggested that NadR has an essential function in *H. influenzae* and probably also in members of *Pasteurella* species. To further differentiate the two enzymatic activities of NadR, RNK and NMNAT, we tested the viability of RNK deletion mutants.

As reported recently (27), a truncated NadR protein consisting of the NMNAT domain is functional in vitro. Here we tested whether the NMNAT NadR alone (with a truncated RNK domain) is sufficient for survival in vivo. For this we constructed *nadR* RNK deletions in an *nadV*$^+$ background (SE01 strain). NadV, a nicotinamide phosphoribosyltransferase (33), allows the cells to utilize Nam by converting it into NMN, thus bypassing the first step of the NadR pathway. SE01ΔRNK was constructed to delete the entire RNK domain (the C-terminal 185 amino acids) (for details see Materials and Methods). The *nadR*ΔRNK::*cat* mutation could be introduced into the SE01 strain (*nadV*$^+$), and the cells were viable on BHI medium without an additional NR source, since the Nam present in BHI broth was sufficient for growth. A second mutation, *nadR*Δ58RNK::*cat*, was constructed and resulted in a 58-amino-acid deletion at the C terminus, which affected the LID structure but left the Walker A (P-loop) and B region intact. This mutation could also be introduced into the chromosome of strain SE01.

To test if NMNAT is sufficient for survival of *H. influenzae*, we used chromosomal DNA derived from strain SE01ΔRNK and transformed it into AK01 (Rd) and, as a control, into SE01 (*nadV*$^+$) and AK01/pNadRkan (*nadR*$^+$). The ratios of Cm^r transformants of AK01 to SE01 and the ratios of Cm^r transformants of AK01 to AK01/pNadRkan were about 1/400. For the Cm^r AK01 colonies, we found that in all transformants tested the *nadR*ΔRNK::*cat* and *nadV*$^+$ gene alleles were concomitantly integrated into the chromosomes, as indicated by the ability of the organisms to grow on BHI medium without an NR source. It was also not possible to isolate *nadR*Δ58::*cat* insertions in the AK01 background without a transfer of *nadV*$^+$ at the same time (data not shown), which led to the transformation frequency of AK01 obtained compared with SE01 or AK01/pNadRkan. These results prove that the RNK domain and the C-terminal 58 amino acids of NadR are essential for the viability of *H. influenzae.*

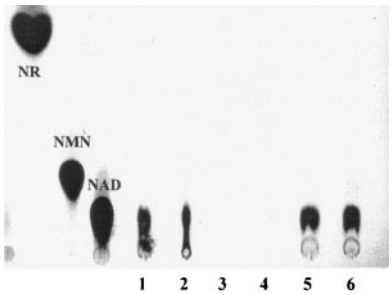

FIG. 1. In vivo NAD$^+$ synthesis. Intact cells were incubated with [^{14}C]NR, and the lysates were subjected to TLC. The positions of nucleosides NR, NMN, and NAD are indicated on the left. Lanes 1 and 2, lysate of AK01 (wild type) after 2 and 30 min of incubation; lanes 3 and 4, lysate of SE01ΔRNK (*nadV*$^+$, RNK$^-$) after 2 and 30 min of incubation; lanes 5 and 6, lysate of SE01ΔRNK/pNadRkan (*nadV*$^+$, RNK$^-$, *nadR*$^+$) after 2 and 30 min of incubation.

RNK deletion mutant and NAD$^+$ synthesis in vivo. The SE01ΔRNK strain was tested for RNK and NMNAT activity and compared with the SE01 wild-type strain and SE01ΔRNK complemented with pNadRkan. The activities were assessed in intact cells and in cell lysates. In assays with intact cells when [^{14}C]NR was used as the substrate, no NAD$^+$ was observed for the SE01ΔRNK mutant (Fig. 1, lanes 3 and 4), whereas the SE01 and the complemented mutant produced NAD$^+$ (Fig. 1). This result led to the conclusion that presumably no [^{14}C]NR label was taken up in a ΔRNK mutant, as shown below. To further test if the NMNAT activity remained intact in the mutant, we added [^{14}C]Nam as a substrate to intact cells. Mutant cells could produce NAD$^+$ from Nam (data not shown), indicating that the NMNAT of NadR in an *nadV*$^+$ background was active in this *nadR*ΔRNK::*cat* mutant.

Characterization of the NadR RNK domain in vitro. To further resolve the properties of the RNK domain, we performed site-directed mutagenesis by targeting the Walker A motif (P-loop), replacing G^{238} with N and S; the Walker B motif, replacing D^{304} with C, N, and S; and the LID region, replacing R^{352} with A, C, M, and N. In particular, we studied NR phosphorylation and NMNAT activities. To characterize the effects of these mutations in vitro and subsequently under in vivo conditions (see below), *nadR* constructs were generated using a commercially available His-tagged expression system (see Materials and Methods). The purified recombinant proteins were tested for activity. The TLC profiles revealed that point mutations in the Walker A (G^{238}) and B (D^{304}) motifs led to inactivation of the RNK activity by preventing NR phosphorylation (Fig. 2, lanes 14 and 15 and lanes 12 and 13,

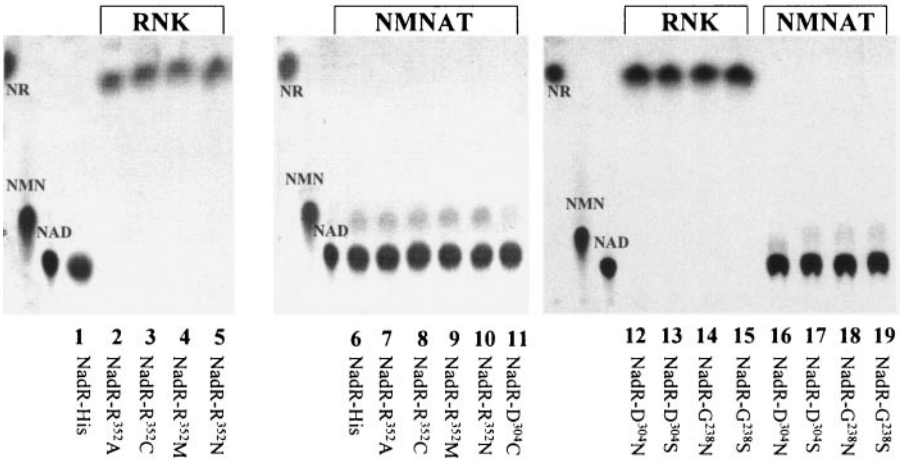

FIG. 2. Mutant analysis of recombinant NadR in vitro. NadR His-tagged and site-directed mutated proteins were purified and used under in vitro conditions for NAD^+ biosynthesis. Recombinant NadR proteins were tested for both RNK and NMNAT activities by TLC analysis. The results for RNK activity were obtained by using [^{14}C]NR in lanes 1 to 5 and 12 to 15, and the results for NMNAT activity were obtained by using [^{14}C]NMN in lanes 6 to 11 and 16 to 19. The NadR-His mutant forms are indicated at the bottom.

respectively). The recombinant NadR gene products with mutations in the putative LID domain (R^{352}) were also negative for RNK activity (Fig. 2, lanes 2 to 5). The mutations generated in R^{352} probably affected the ability of the enzyme to form an enzyme-substrate complex, as shown previously for other LID domain-associated enzymes (30, 31, 41, 49). Testing the NMNAT activity (Fig. 2, lanes 6 to 11 and 16 to 19) demonstrated that all mutant NadR proteins were able to synthesize NAD^+; therefore, disrupting the RNK activity had no effect on the action of NMNAT.

NR transport in RNK mutants. To address the question of the involvement of the RNK domain in NR transport, the rate of accumulation of [^{14}C]NR derived from [^{14}C]NAD uptake over time was determined for SE01ΔRNK and for mutants with point mutations in *nadR* located in the Walker A and B and LID regions. To do this, the point mutations were transferred onto the chromosome. The results showed that the uptake of [^{14}C]NAD was only about 2 to 5% in SE01ΔRNK, compared to the 60 and 80% observed for SE01ΔRNK/pNadRKan and SE01, respectively (Fig. 3). The RNK mutated NadR His-tagged constructs were expressed in strain SE01ΔRNK, and the NR transport phenotype was characterized under in vivo conditions. All point mutations affecting NR phosphorylation in vitro (see above) were accompanied by a significant decrease in [^{14}C]NR uptake in vivo (Table 3). This indicates that NR phosphorylation via NadR also appears to be essential for transport. Interestingly, the D^{304}C and D^{304}N mutations, but not D^{304}S, resulted in attenuated NR transport activities; this may suggest that there was some residual low level of NR phosphorylation, but this could be not confirmed (e.g., for D^{304}N) (Fig. 2).

Cellular localization of the NadR protein and NadR activities. Cell fractionation and immunoblot analysis (Fig. 4) revealed that native NadR was present in soluble as well as membrane fractions. NadR activities were retained in the membrane fractions (Fig. 5). Treatment with 1 M NaCl resulted in partial dissociation of NadR from the membranes, indicating that there was an association between NadR and cytosolic membranes. Triton X-100 (2%) solubilized less NadR than NaCl treatment, and no differences in NadR localization were observed in the presence and absence of PnuC (data not shown). Similar results were also found for the point mutants tested (data not shown). Singh et al. (46) indicated that NadR seems to form a homotetramer. We do not know whether conformational changes take place and whether different conformations can be found in cytosolic or membrane fractions. However, we deduced from our analysis that a functional RNK domain does not seem to be necessary for membrane association but may have a profound effect on protein stability, since ΔRNK forms of NadR (i.e., the forms in strains SE01ΔRNK and SE01*nadR*Δ58::*cat*) were not visible in the immunoblot analysis (data not shown).

NadR feedback regulation and NR uptake. Crystallography of NadR revealed that NAD^+ cocrystallized with NadR at nonactive sites within the RNK domain (46). To test whether

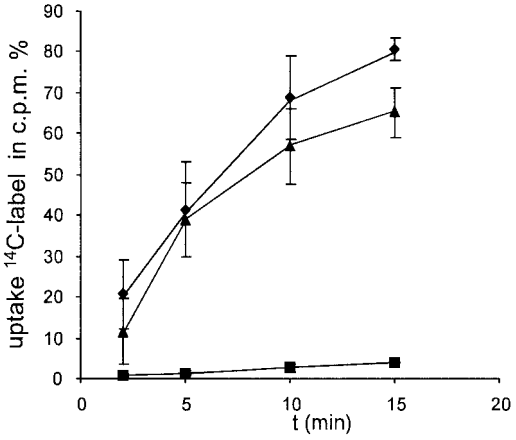

FIG. 3. Effect of *nadR*ΔRNK on the uptake of ^{14}C-labeled substrate derived from [^{14}C]NAD^+: uptake of ^{14}C-labeled substrate by SE01 (wild type) (◆), SE01ΔRNK (■), and SE02ΔRNK/pNadRKan (▲). The uptake of the ^{14}C label was expressed as the intracellular accumulation of cpm derived from [^{14}C]NAD provided in the growth medium (100%). The standard deviations indicated by the error bars were based on three independent measurements.

TABLE 3. Transport ability of NadR RNK point mutations in *H. influenzae*[a]

Strain	Mutation	Uptake of ^{14}C label (%)	SD
SE01	Wild type	65.1	6.250
SE01ΔRNK	ΔRNK	3.1	0.565
SE02ΔRNK	NadR-His_6	70.0	7.587
SE03ΔRNK	$G^{238}N$	4.8	2.375
SE04ΔRNK	$G^{238}S$	5.8	0.799
SE05ΔRNK	$D^{304}C$	16.3	2.354
SE06ΔRNK	$D^{304}N$	19.3	0.289
SE07ΔRNK	$D^{304}S$	4.5	3.394
SE08ΔRNK	$R^{352}C$	4.4	1.237
SE09ΔRNK	$R^{352}M$	3.4	1.414
SE10ΔRNK	$R^{352}N$	6.0	0.424

[a] The values indicate the accumulation of [^{14}C]NAD^+-derived substrate for strains SE01ΔRNK to SE10ΔRNK (Table 1) having point mutants in *nadR*. The uptake of the ^{14}C label indicates the intracellular accumulation of cpm derived from [^{14}C]NAD provided in the growth medium (100%). The standard deviations are based on three independent measurements.

NAD^+, as a product of NadR, feedback controls NadR activity, we incubated purified NadR-His_6 with [^{14}C]NR or [^{14}C]NMN and with a 200-fold excess of NAD^+ (9 mM) and determined the RNK and NMNAT activities by TLC analysis. The results show that the RNK activity was significantly reduced in the presence of NAD^+ (Fig. 6A and B), whereas the NMNAT activity was only slightly affected (Fig. 6A and C). Quantification of the reaction in the presence of different NAD^+ concentrations showed that increased NAD^+ concentrations reduced the RNK activity gradually, as shown in Fig. 6B, but not the NMNAT activity (Fig. 6C).

In order to test whether NAD^+ utilization is controlled by NAD^+ feedback mechanisms, cells were incubated with and without NAD^+ (15 μM) in a preincubation phase prior to washing and analysis. By comparing the two conditions, we found a threefold reduction in the uptake rate over time for [^{14}C]NAD^+-derived [^{14}C]NR accumulation (Fig. 7).

To further address the question of feedback inhibition of NadR by NAD^+, amino acids K^{126}, W^{256}, and Y^{292} were changed to K^{126}A/T, W^{256}F, and Y^{292}I. These amino acids were suggested to interact with non-active-site-bound NAD^+ (46), but there was no experimental proof for this. The mutated and recombinant expressed NadR His-tagged proteins were purified, and the reaction was monitored in vitro. As a result, we found that the amino acid change K^{126}A or K^{126}T resulted in a significant reduction in RNK activity and also impairment of the NMNAT activity in an assay using protein concentrations of 0.04 mg/ml (data not shown). The Y^{292}I change worked well for the RNK and NMNAT activity assay when 0.04 mg/ml was used but was deficient at lower protein concentrations compared with NadR-His. However, the activity after the W^{256}F change was comparable to the NadR-His activity under standard reaction conditions (0.04 mg/ml), but a less responsive NAD^+ feedback inhibition effect was observed (Fig. 8). In a semiquantitative analysis, in which we monitored the product [^{14}C]NAD^+ (by determining the cpm for [^{14}C]NAD^+ spots derived from TLC plates [Fig. 8]) (for instance, at 80 min), an inhibition level of 4% was found for W^{256}F NadR-His, compared with the 80% inhibition of NadR-His activity. The level of inhibition was calculated by determining the ratio of the cpm derived from reactions with unlabeled NAD^+ (9 mM) to the cpm derived from reactions without unlabeled NAD^+.

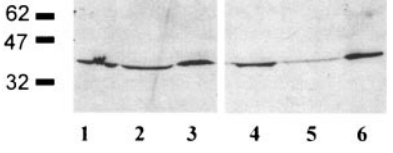

FIG. 4. Cellular localization of native NadR: immunoblot analysis with polyclonal anti-NadR serum (see Materials and Methods). The amount of protein used was 60 μg for all fractions except the NaCl fraction (40 μg). Lane 1, crude cell fraction; lane 2, soluble fraction; lane 3, membrane pellet; lane 4, supernatant after NaCl (1 M) treatment of the membrane pellet; lane 5, supernatant after Triton X-100 (2%) treatment of the membrane pellet; lane 6, nonsoluble membrane pellet. The positions of molecular mass protein standards (New England Biolabs) (in kilodaltons) are indicated on the left.

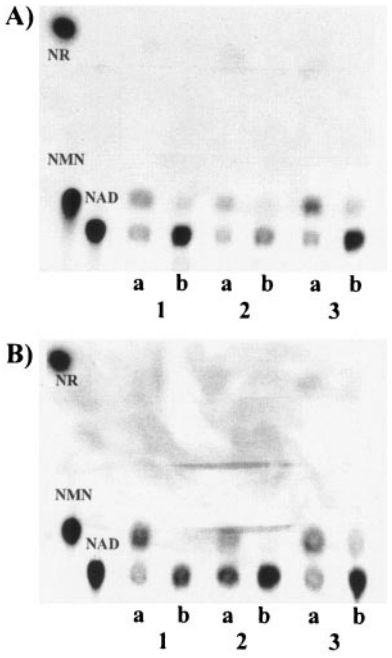

FIG. 5. NadR localization and activity. Cell fractions were incubated with [^{14}C]NR (A) or with [^{14}C]NMN (B) for either 5 min (lanes a) or 30 min (lanes b), and samples were subjected to TLC. Lanes 1, crude extract; lanes 2, soluble extract; lanes 3, membrane fraction.

DISCUSSION

H. influenzae probably arrived at an evolutionary bottleneck, reflected by significant genome reduction and strict host dependence (25). NAD^+ biosynthesis deficiency is one characteristic of *H. influenzae* which makes this organism dependent on host nicotinamide sources, and NadR seems to play an essential role (13, 27). Therefore, in this study we aimed to further characterize NadR, a putative target protein for the development of a novel antimicrobial treatment. Considering the Nam and NR dependence, deduced from the genomic information for some members of the family *Pasteurellaceae*, the NadR/PnuC or NadR/NadV pathways are probably the only routes for recovering NAD^+ from a mammalian host. The

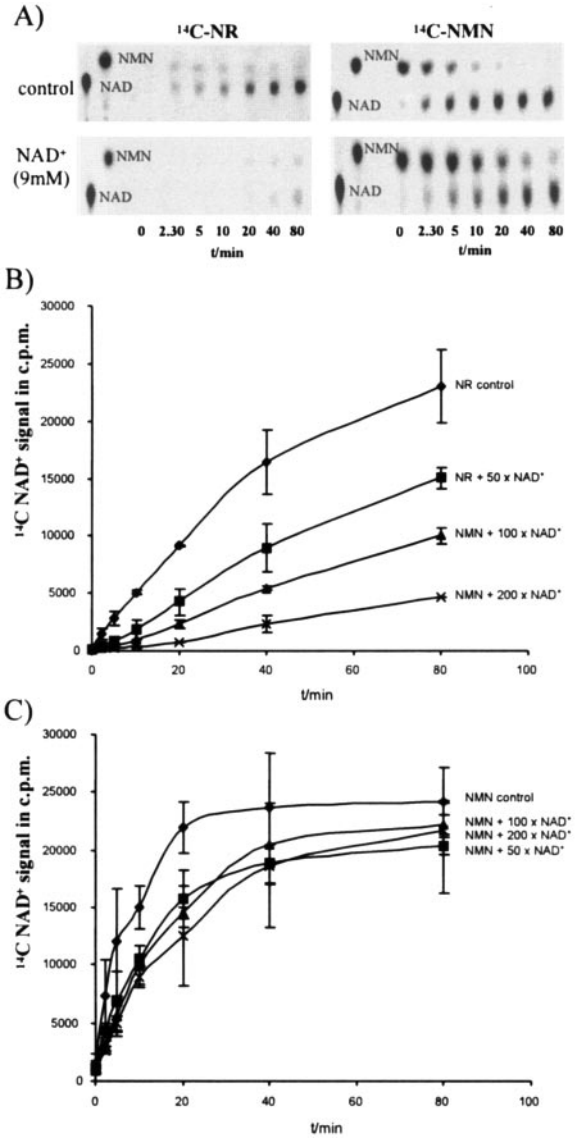

FIG. 6. NAD+-mediated inhibition of NadR activity. (A) NAD+ synthesis with purified recombinant NadR His-tagged protein was analyzed by TLC (see Materials and Methods). (Left panel) [14C]NR substrate without and with unlabeled NAD+ (9 mM) for 0 to 80 min. (Right panel) [14C]NMN substrate without and with unlabeled NAD+ (9 mM) for 0 to 80 min. (B) Inhibition of the RNK activity dependent on different NAD+ concentrations at 0 to 80 min. (C) Inhibition of the NMNAT activity dependent on different NAD+ concentrations at 0 to 80 min. The analysis was performed as described in Materials and Methods. Briefly, [14C]NAD+-containing spots on TLC plates were cut out and counted with a Tri-Carb 1500 scintillation counter. The standard deviations indicated by the error bars were based on two independent measurements.

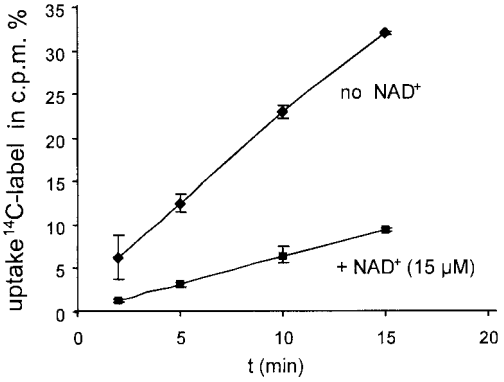

FIG. 7. NAD+ utilization with NAD+ preincubation. The strain used was AK01, and [14C]NAD+ accumulation was determined over time. An AK01 culture was divided and washed, and one sample was incubated in BHI medium with unlabeled NAD+ (15 μM) (■) and the other sample was incubated in BHI medium alone (◆). Cells were then washed in fresh BHI medium and resuspended in BHI medium; subsequently, [14C]NAD+ (1 μM) was added. Accumulation was determined by filtering the cells and determining the incorporated radioactivity. The uptake of the 14C label was expressed as the accumulation of intracellular cpm derived from [14C]NAD provided in the growth medium (100%). The standard deviations indicated by the error bars were based on three independent measurements.

biochemical properties of NadR of *H. influenzae* (*hi*NadR) and NadR of *S. enterica* serovar Typhimurium (*st*NadR) reveal some interesting differences. *st*NadR can act as an NAD+-responsive transcriptional regulator, harboring an N′-terminal helix-turn-helix motif and recognizing operator sites termed "NAD boxes" (37). *st*NadR acts as an important control circuit component for NAD+ biosynthesis, regulating the transcription of genes encoding enzymes used for de novo NAD+ synthesis (*nadAB*) and nicotinic acid recycling (*pncB*). *st*NadR becomes a repressor at a cellular NAD+ concentration around 1 mM, while at lower NAD+ concentrations the repressor function is abolished (20, 37). *hi*NadR lacks the helix-turn-helix region, which commits it to NAD+ synthesis only (27). A comparison of in vitro biochemical properties of *hi*NadR and *st*NadR showed that *hi*NadR has been optimized for NAD+ formation (e.g., by having approximately 22-fold greater NMNAT activity than *st*NadR) (27). However, based on a comparison of the RNK activities, *st*NadR seems to have significantly higher activity. Overall, these results may indicate that there is a minor flux via NadR to the NAD+ pool in the *Enterobacteriaceae*, while de novo biosynthesis and pyridine nucleotide salvage pathways operate (27).

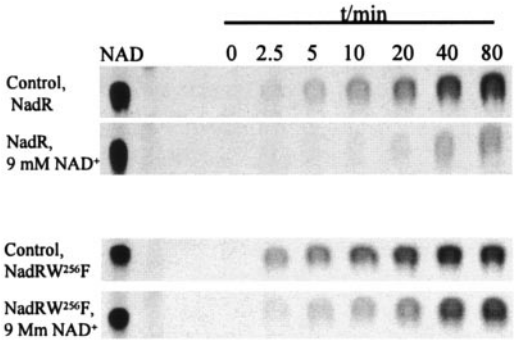

FIG. 8. NAD+ feedback inhibition with NadR-His and NadRW256F-His: sections of TLCs showing NAD+ synthesis with [14C]NR as the substrate with and without unlabeled NAD+. At different time samples were taken and analyzed by TLC. The upper two rows show the results for reactions performed with NadR-His, and the lower two rows show the results for reactions performed with NadRW256F-His. An NAD+ control sample was included, and the results obtained are indicated on the left.

With research directed at determining the in vivo role of *hi*NadR, we unraveled the essential functions of NadR represented by two domains, NMNAT and RNK. With a combination of transformation experiments, we demonstrated that an *nadR*ΔRNK mutation could only be introduced into the chromosome of *H. influenzae nadV*$^+$ or cells harboring *nadR*$^+$ on a plasmid. This demonstrated that not only the NMNAT activity but also the RNK activity of NadR is essential for survival. In addition, these experiments showed that in the presence of NadV, the RNK activity is redundant and not essential, which should be the case for other *Pasteurellaceae* species that harbor *nadV*, including *Pasteurella multocida*, *Actinobacillus actinomycetemcomitans*, and *H. ducreyi*. NadV corresponds to PncB in *S. enterica* serovar Typhimurium. In that organism, PncB is a key enzyme for nicotinic acid scavenging and catalyzes the formation of nicotinic acid mononucleotide from nicotinic acid, phosphoribosylpyrophosphate, and ATP (51, 53). Regulation of PncB activity is achieved by autophosphorylation of PncB depending on the cellular ATP level (50). Whether NadV is regulated by a similar mechanism is not known.

As reported here, mutants with site-directed mutations in the Walker A and B and LID motifs of NadR showed no RNK activity under in vitro conditions, but the NMNAT activity remained intact. This finding is consistent with data presented previously which showed that NMNAT activity in vitro was derived from a partial NadR protein (N′-terminal half) lacking the RNK domain (27). By testing site-directed mutations of *nadR* in *H. influenzae* in vivo, we found that all mutants caused an NR transport deficiency, which was also observed for the *nadR*ΔRNK mutant. As reported previously (11, 12, 56), *nadR* mutations in *S. enterica* serovar Typhimurium, which resulted in a marked decrease in NMN uptake, mapped in the C′ terminus, but the molecular details were not resolved. These early observations were confirmed and extended with our data, which showed that this effect correlates with disruption of the NadR RNK activity. This result also shed new light on the mechanism of NR uptake by PnuC. PnuC acts specifically as an NR permease in *H. influenzae*, and as recently shown by us, PnuC derived from *E. coli* also acts as an NR permease with no specificity for NMN. Hence, we postulated that all PnuC homologous transporters probably act as NR permeases (42). Previous approaches (6) indicated that ATP depletion but not disruption of the proton motive force decreased NR uptake in *Haemophilus*; hence, it is assumed that PnuC is related to uniport-based permease systems. A well-investigated uniport system is represented by the glycerol facilitator channel GlpF of *E. coli* (48). In this organism, the glycerol kinase seems to direct the substrate flow direction by phosphorylating glycerol in the cell, hindering glycerol efflux. An interaction between the kinase and permease was suggested (52). Our data also suggest that NR phosphorylation by NadR is the driving force for PnuC-mediated NR transport. A concerted activity could be envisaged, in which NadR facilitates the dissociation of NR from PnuC by phosphorylating it to NMN, thus preventing retrograde diffusion (efflux) of NR. The fact that NadR can be found as a soluble cytosolic protein as well as a membrane-associated protein may indicate that NadR and PnuC are in close proximity, which is necessary to promote NR influx and to prevent efflux. If this is true, then substrate flow across the membrane is coupled to the rate of NR phosphorylation. At this point it is not clear whether the permease or the NadR activity is rate limiting for substrate flow.

As reported recently, by using NadR structure resolution (46) several specific interaction sites were found with a non-active-site NAD^+ molecule bound between W^{256} and Y^{292}. In the established protein structure, interaction of NAD^+ with K^{126}, W^{256}, and Y^{289} of the tetrameric conformation model of NadR was suggested, which led to the idea of biological consequences (46). NAD^+ binding to *st*NadR was postulated to switch the NadR conformation to an active repressor form (36). Recently, it was shown that NAD^+ binding to *st*NadR makes it active for binding to "NAD boxes" of the *nadA* operator region (37). We also investigated whether RNK and NMNAT are under feedback control by the end product NAD^+. Feedback inhibition was observed mainly for RNK in vitro, and indirectly we showed that the NR uptake rate is influenced by NAD^+ depletion under in vivo conditions. Furthermore, we constructed point mutations, addressing the non-active NAD^+ binding site. The amino acid change $W^{256}F$ resulted in an NadR mutant protein which was less affected in the presence of the inhibitor NAD^+ than NadR-His under in vitro conditions. This indicates that W^{256} has an important role in the interaction with NAD^+ and that this amino acid might be involved in forwarding feedback inhibition in an allosteric way to the reactive centers of NadR. Interestingly, the other mutations, especially the change at K^{126} to T or A, impaired the RNK function, although they were not located in the Walker A or B or LID motif. Further analysis is necessary to more specifically assign a role to these amino acids in enzyme activity and feedback inhibition. Consequently, it seems that feedback regulation controls NR uptake and NR phosphorylation mainly by regulating the RNK activity, which is mediated by intracellular NAD^+ concentrations.

The biological half-life of NAD^+ in bacterial cells grown aerobically is about 90 min (35); thus, there is NAD^+ turnover, and pyridine nucleotide cycles have been identified (36). Within these cycles a few control points for regulation have been identified, such as those described for NadR and PncB. Other activities, such as NAD or NMN glycohydrolases, have been described for several organisms, including *H. influenzae* (6, 37). However, to our knowledge, no corresponding gene products which have a physiological role in cellular NAD^+ turnover have been identified. There is one open reading frame, annotated as a NUDIX motif harboring NADH pyrophosphorylase (HI0432) (9), which might have a role in NADH turnover. So far, a mutant of HI0432 has been isolated and has been found to be attenuated in the infant rat infection model; however, there is no direct evidence concerning its function (17). Since in *H. influenzae* NadR does not have a repressor function (27) and no pyridine nucleotide cycles are present (9), it seems unlikely that the transcriptional regulation feedback systems observed in *S. enterica* serovar Typhimurium and in *E. coli* work in *H. influenzae*. A final conclusion of this work, therefore, is that *hi*NadR is the key component for both NAD^+ synthesis and control of the NAD^+ biosynthesis rate in *H. influenzae*.

ACKNOWLEDGMENTS

This work was supported by Deutsche Forschungsgemeinschaft grant RE1561/1-2.

We are grateful to S. Schild for providing plasmid pSSkan. We thank W. Vollmer and M. Herbert for suggestions and critical reading of the manuscript.

REFERENCES

1. **Akerley, B. J., E. J. Rubin, V. L. Novick, K. Amaya, N. Judson, and J. J. Mekalanos.** 2002. A genome-scale analysis for identification of genes required for growth or survival of *Haemophilus influenzae*. Proc. Natl. Acad. Sci. USA **99:**966–971.
2. **Andersen, C., E. Maier, G. Kemmer, J. Blass, A. K. Hilpert, R. Benz, and J. Reidl.** 2003. Porin OmpP2 of *Haemophilus influenzae* shows substrate specificity towards nicotinamide-derived nucleotide substrates. J. Biol. Chem. **278:**24269–24276.
3. **Barcak, G. J., M. S. Chandler, R. J. Redfield, and J. F. Tomb.** 1991. Genetic systems in *Haemophilus influenzae*. Methods Enzymol. **204:**321–342.
4. **Bieganowski, P., and C. Brenner.** 2004. Discoveries of nicotinamide riboside as a nutrient and conserved NRK genes establish a Preiss-Handler independent route to NAD^+ in fungi and humans. Cell **117:**495–502.
5. **Bradford, M. M.** 1976. A rapid and sensitive method for the quantitation of microgram quantities of protein utilizing the principle of protein-dye binding. Anal. Biochem. **72:**248–254.
6. **Cynamon, M. H., T. B. Sorg, and A. Patapow.** 1988. Utilization and metabolism of NAD by *Haemophilus parainfluenzae*. J. Gen. Microbiol. **134:**2789–2799.
7. **Denicola-Seoane, A., and B. M. Anderson.** 1990. Studies of NAD kinase and NMN:ATP adenylyltransferase in *Haemophilus influenzae*. J. Gen. Microbiol. **136:**425–430.
8. **Evans, N. M., D. D. Smith, and A. J. Wicken.** 1974. Hemin and nicotinamide adenine dinucleotide requirements of *Haemophilus influenzae*. J. Med. Microbiol. **7:**359–365.
9. **Fleischmann, R. D., M. D. Adams, O. White, R. A. Clayton, E. F. Kirkness, A. R. Kerlavage, C. J. Bult, J. F. Tomb, B. A. Dougherty, J. M. Merrick, K. McKenney, G. Sutton, W. F. Hugh, C. Fields, J. D. Gocayne, J. Scott, R. Shirley, L. I. Liu, A. Glodek, J. M. Kelley, J. F. Weidman, C. A. Phillips, T. Spriggs, E. Hedblom, M. D. Cotton, T. R. Utterback, M. C. Hanna, D. T. Nguyen, D. M. Saudek, R. C. Brandon, L. D. Fine, J. L. Frichman, J. L. Fuhrmann, N. S. M. Geoghagen, C. L. Gnehm, L. A. McDonald, K. V. Small, C. M. Fraser, H. O. Smith, and J. C. Venter.** 1995. Whole-genome random sequencing and assembly of *Haemophilus influenzae* Rd. Science **269:**496–512.
10. **Foster, J. W., E. A. Holly-Guthrie, and F. Warren.** 1987. Regulation of NAD metabolism in *Salmonella typhimurium*: genetic analysis and cloning of the *nadR* repressor locus. Mol. Gen. Genet. **208:**279–287.
11. **Foster, J. W., Y. K. Park, T. Penfound, T. Fenger, and M. P. Spector.** 1990. Regulation of NAD metabolism *in Salmonella typhimurium*: molecular sequence analysis of the bifunctional *nadR* regulator and the *nadA-pnuC* operon. J. Bacteriol. **172:**4187–4196.
12. **Foster, J. W., and T. Penfound.** 1993. The bifunctional NadR regulator of *Salmonella typhimurium*: location of regions involved with DNA binding, nucleotide transport and intramolecular communication. FEMS Microbiol. Lett. **112:**179–184.
13. **Gerdes, S. Y., M. D. Scholle, M. D'Souza, A. Bernal, M. V. Baev, M. Farrell, O. V. Kurnasov, M. D. Daugherty, F. Mseeh, B. M. Polanuyer, J. W. Campbell, S. Anantha, K. Y. Shatalin, S. A. K. Chowdhury, M. Y. Fonstein, and A. L. Osterman.** 2002. From genetic footprinting to antimicrobial drug targets: examples in cofactor biosynthetic pathways. J. Bacteriol. **184:**4555–4572.
14. **Gingrich, W., and F. Schlenk.** 1944. Codehydrogenase I and other pyridinium compounds as V factor for *Haemophilus influenzae* and *Haemophilus parainfluenzae*. J. Bacteriol. **47:**535–550.
15. **Grimberg, J., S. Maguire, and L. Belluscio.** 1989. A simple method for the preparation of plasmid and chromosomal *E. coli* DNA. Nucleic Acids Res. **17:**8893.
16. **Guzman, L. M., D. Belin, M. J. Carson, and J. Beckwith.** 1995. Tight regulation, modulation, and high-level expression by vectors containing the arabinose pBAD promoter. J. Bacteriol. **177:**4121–4130.
17. **Herbert, M. A., S. Hayes, M. E. Deadman, C. M. Tang, D. W. Hood, and E. R. Moxon.** 2002. Signature tagged mutagenesis of *Haemophilus influenzae* identifies genes required for in vivo survival. Microb. Pathog. **33:**211–223.
18. **Herbert, M. A., A. Kraiß, A.-K. Hilpert, and J. Reidl.** 2003. Aerobic growth deficient *Haemophilus influenzae* mutants are non-virulent in the rat model: implications on metabolism. J. Int. Med. Microbiol. **293:**145–152.
19. **Herbert, M. A., E. Sauer, G. Smethurst, A. Kraiß, A.-K. Hilpert, and J. Reidl.** 2003. Identification and characterization of nicotinamide-ribosyl uptake mutants in *Haemophilus influenzae*. Infect. Immun. **71:**5398–5401.
20. **Holley, E. A., M. P. Spector, and J. W. Foster.** 1985. Regulation of NAD biosynthesis in *Salmonella typhimurium*: expression of *nad-lac* gene fusions and identification of a *nad* regulatory locus. J. Gen. Microbiol. **131:**2759–2770.
21. **Kahn, D. W., and B. M. Anderson.** 1986. Characterization of *Haemophilus influenzae* nucleotide pyrophosphatase. J. Biol. Chem. **261:**6016–6025.
22. **Kasarov, L. B., and A. G. Moat.** 1972. Convenient method for enzymatic synthesis of ^{14}C-nicotinamide riboside. Anal. Biochem. **46:**181–186.
23. **Kemmer, G., T. Reilly, J. Schmidt-Brauns, G. W. Zlotnik, B. A. Green, M. J. Fiske, M. Herbert, A. Kraiß, S. Schlör, A. Smith, and J. Reidl.** 2001. NadN and *e* (P4) are essential for the utilization of NAD and nicotinamide mononucleotide but not nicotinamide riboside in *Haemophilus influenzae*. J. Bacteriol. **183:**3974–3981.
24. **Kilian, M.** 1991. *Haemophilus*, p. 463–470. *In* A. Balows, W. J. Hausler, Jr., K. L. Herrmann, H. D. Isenberg, and H. J. Shadomy (ed.), Manual of clinical microbiology, 5th ed. American Society for Microbiology, Washington, D.C.
25. **Koonin, E. V.** 2000. How many genes can make a cell: the minimal-gene-set concept. Annu. Rev. Genomics Hum. Genet. **1:**99–116.
26. **Kraiß, A., J. Blaß, and J. Reidl.** 1998. A suicide plasmid (pJR*lacZ*ins) for targeted integration of non-native genes into the chromosome of *Escherichia coli*. Trends Microbiol. **6:**10.
27. **Kurnasov, O. V., B. M. Polanuyer, S. Ananta, R. Sloutsky, A. Tam, S. Y. Gerdes, and A. L. Osterman.** 2002. Ribosylnicotinamide kinase domain of NadR protein: identification and implications in NAD biosynthesis. J. Bacteriol. **184:**6906–6917.
28. **Laemmli, U. K.** 1970. Cleavage of structural proteins during the assembly of the head of bacteriophage T4. Nature **227:**680–685.
29. **Lavie, A., M. Konrad, R. Brundiers, R. S. Goody, I. Schlichting, and J. Reinstein.** 1998. Crystal structure of yeast thymidylate kinase complexed with the bisubstrate inhibitor P1-(5′-adenosyl) P5-(5′-thymidyl) pentaphosphate (TP5A) at 2.0 A resolution: implications for catalysis and AZT activation. Biochemistry **37:**3677–3686.
30. **Lavie, A., N. Ostermann, R. Brundiers, R. S. Goody, J. Reinstein, M. Konrad, and I. Schlichting.** 1998. Structural basis for efficient phosphorylation of 3′-azidothymidine monophosphate by *Escherichia coli* thymidylate kinase. Proc. Natl. Acad. Sci. USA **95:**14045–14050.
31. **Li de la Sierra, I., H. Munier-Lehmann, A. M. Gilles, O. Barzu, and M. Delarue.** 2001. X-ray structure of TMP kinase from *Mycobacterium tuberculosis* complexed with TMP at 1.95 A resolution. J. Mol. Biol. **311:**87–100.
32. **Lutz, R., and H. Bujard.** 1997. Independent and tight regulation of transcriptional units in *Escherichia coli* via the LacR/O, the TetR/O and AraC/I1–I2 regulatory elements. Nucleic Acids Res. **25:**1203–1210.
33. **Martin, P. R., R. J. Shea, and M. H. Mulks.** 2001. Identification of a plasmid-encoded gene from *Haemophilus ducreyi* which confers NAD independence. J. Bacteriol. **183:**1168–1174.
34. **Muller, C. W., G. J. Schlauderer, J. Reinstein, and G. E. Schulz.** 1996. Adenylate kinase motions during catalysis: an energetic counterweight balancing substrate binding. Structure **15:**147–156.
35. **Park, U. E., B. M. Olivera, K. T. Hughes, J. R. Roth, and D. R. Hillyard.** 1989. DNA ligase and the pyridine nucleotide cycle in *Salmonella typhimurium*. J. Bacteriol. **171:**2173–2180.
36. **Penfound, T., and J. W. Foster.** 1996. Biosynthesis and recycling of NAD, p. 721–730. *In* F. C. Neidhardt, R. Curtis III, J. L. Ingraham, E. C. C. Lin, K. B. Low, B. Magasanik, W. S. Reznikoff, M. Riley, M. Schaechter, and H. E. Umbarger (ed.), *Escherichia coli* and *Salmonella*: cellular and molecular biology, 2nd ed., vol. 1. American Society for Microbiology Washington, D.C.
37. **Penfound, T., and J. W. Foster.** 1999. NAD-dependent DNA binding activity of the bifunctional NadR regulator of *Salmonella typhimurium*. J. Bacteriol. **181:**648–655.
38. **Raffaelli, N., P. L. Lorenzi, M. Emanuelli, A. Amici, S. Ruggieri, and G. Magni.** 1999. The *Escherichia coli* NadR regulator is endowed with nicotinamide mononucleotide adenylytransferase activity. J. Bacteriol. **181:**5509–5511.
39. **Redfield, R. J.** 1991. *sxy-1*, a *Haemophilus influenzae* mutation causing greatly enhanced spontaneous competence. J. Bacteriol. **173:**5612–5618.
40. **Reidl, J., S. Schlör, A. Kraiss, J. Schmidt-Brauns, G. Kemmer, and E. Soleva.** 2000. NADP and NAD utilization in *Haemophilus influenzae*. Mol. Microbiol. **35:**1573–1581.
41. **Rombel, I., P. Peters-Wendisch, A. Mesecar, T. Thorgeirsson, Y. K. Shin, and S. Kustu.** 1999. MgATP binding and hydrolysis determinants of NtrC, a bacterial enhancer-binding protein. J. Bacteriol. **181:**4628–4638.
42. **Sauer, E., M. Merdanovic, A. Price Mortimer, G. Bringmann, and J. Reidl.** 2004. Characterizing PnuC and the utilization of the nicotinamide riboside analog 3-aminopyridine in *Haemophilus influenzae*. Antimicrob. Agents Chemother. **48:**4532–4541.
43. **Saunders, P. P., M. T. Tan, C. D. Spindler, and R. K. Robins.** 1989. Phosphorylation of 3-deazaguanosine by nicotinamide riboside kinase in Chinese hamster ovary cells. Cancer Res. **49:**6593–6599.
44. **Schmidt-Brauns, J., M. Herbert, G. Kemmer, A. Kraiß, S. Schlör, and J. Reidl.** 2001. Is a NAD-pyrophosphatase activity needed by *Haemophilus influenzae* type b for multiplication in the blood stream? Int. J. Med. Microbiol. **291:**219–225.
45. **Shifrine, M., and E. L. Biberstein.** 1960. A growth factor for *Haemophilus* species secreted by a pseudomonad. Nature **187:**623.
46. **Singh, S. K., O. V. Kurnasov, B. Chen, H. Robinson, N. V. Grishin, A. L. Osterman, and H. Zhang.** 2002. Crystal structure of *Haemophilus influenzae* NadR protein: a bifunctional enzyme endowed with NMN adenylyltrans-

ferase and ribosylnicotinamide kinase activities. J. Biol. Chem. **277:**33291–33299.
47. **Southern, E. M.** 1975. Detection of specific sequences among DNA fragments separated by gel electrophoresis. J. Mol. Biol. **51:**503–517.
48. **Sweet, G., C. Gandor, R. Voegele, N. Wittekindt, J. Beuerle, V. Truniger, E. C. Lin, and W. Boos.** 1990. Glycerol facilitator of *Escherichia coli*: cloning of *glpF* and identification of the *glpF* product. J. Bacteriol. **172:**424–430.
49. **Via, A., F. Ferre, B. Brannetti, A. Valencia, and M. Helmer-Citterich.** 2000. Three-dimensional view of the surface motif associated with the P-loop structure: cis and trans cases of convergent evolution. J. Mol. Biol. **303:**455–465.
50. **Vinitsky, A., and C. Grubmeyer.** 1993. A new paradigm for biochemical energy coupling. *Salmonella typhimurium* nicotinate phosphoribosyltransferase. J. Biol. Chem. **268:**26004–26010.
51. **Vinitsky, A., H. Teng, and C. T. Grubmeyer.** 1991. Cloning and nucleic acid sequence of the *Salmonella typhimurium pncB* gene and structure of nicotinate phosphoribosyltransferase. J. Bacteriol. **173:**536–540.
52. **Voegele, R. T., G. D. Sweet, and W. Boos.** 1993. Glycerol kinase of *Escherichia coli* is activated by interaction with the glycerol facilitator. J. Bacteriol. **175:**1087–1094.
53. **Wubbolts, M. G., P. Terpstra, J. B. van Beilen, J. Kingma, H. A. Meesters, and B. Witholt.** 1991. Variation of cofactor levels in *Escherichia coli*. Sequence analysis and expression of the *pncB* gene encoding nicotinic acid phosphoribosyltransferase. J. Biol. Chem. **265:**17665–17672.
54. **Yan, H., and M. D. Tsai.** 1999. Nucleoside monophosphate kinases: structure, mechanism, and substrate specificity. Adv. Enzymol. Relat. Areas Mol. Biol. **73:**103–134.
55. **Yanisch-Perron, C., J. Vieira, and J. Messing.** 1985. Improved M13 phage cloning vectors and host strains: nucleotide sequences of the M13mp18 and pUC19 vectors. Gene **33:**103–119.
56. **Zhu, N., B. M. Olivera, and J. R. Roth.** 1991. Activity of the nicotinamide mononucleotide transporter system is regulated in *Salmonella typhimurium*. J. Bacteriol. **173:**1311–1320.